Chemical Engineering Journal 92 (2003) 177–184

Chemical Engineering Journal
www.elsevier.com/locate/cej

Reaction mechanism of 1,2-dichloroethane/O_2/Ar in the cold plasma environment

Chun-Teh Li[a,*], Renbo Yang[a], Minliang Shih[a], Perng-Jy Tsai[d],
Lien-Te Hsieh[b], Chuh-Yung Chen[c]

[a] *Department of Environmental Engineering, National Cheng Kung University, No.1 University Road, Tainan 70101, Taiwan*
[b] *Department of Environmental Engineering and Science, National Pingtung University of Science and Technology,*
No. 1 Hseuh Fu Road, Nei Pu Hsiang, Ping Tung 91201, Taiwan
[c] *Department of Chemical Engineering, National Cheng Kung University, No.1 University Road, Tainan 70101, Taiwan*
[d] *Department of Environmental and Occupational Health, Medical College, National Cheng Kung University,*
No. 138, Sheng-Li Road, Tainan 70428, Taiwan

Abstract

1,2-Dichloroethane (EDC) is known to be hazardous to the environment and public health. In this study, application of radio frequency (rf) plasma as an alternative technology for the decomposition of EDC was demonstrated. The species detected in the effluent gas stream included CO_2, CO, HCl, CCl_4, C_2HCl_3, C_2H_3Cl, C_2Cl_4, $CHCl_3$, C_2HCl_5, $COCl_2$, C_2H_2, C_2H_4, C_2H_6, and HCOOH. The decomposition fraction of EDC $[\eta_{C_2H_4Cl_2}, (C_{in} - C_{out})/C_{in} \times 100\ (\%)]$ was dependent on input power. When input power was 80 W, stable products such as CO, CO_2, and HCl were dominant and other product species were inhibited. Equivalence ratio $[\varphi = (C_2H_4Cl_2/O_2)_{actual} \times (O_2/C_2H_4Cl_2)_{stoichiometric}]$ was the other important operational parameter in a plasma system. When the chlorocarbon/oxygen flow was fuel rich, more soot formation was found in the plasma reactor. When it was fuel lean, CO_2 and CO dominated over other product species. Within the mixture of EDC and dichloromethane (DCM), the competition of DCM with EDC could affect the decomposition fraction of EDC.

Keywords: Decomposition; 1,2-Dichloroethane; Radio frequency (rf); Plasma; Reaction mechanism

1. Introduction

1,2-Dichloroethane (EDC), a precursor to vinyl chloride monomer (VCM) and hence polyvinyl chloride (PVC) of manufacturing processes [1] is known to be hazardous to the environment and public health. Thermal decomposition of EDC has been studied since 1949 [2]. Following this, Holbrook et al. have illustrated that although vinyl chloride was the major reaction product of a homogeneous gas phase reaction, ethene was another primary reaction product [3]. Walter and Jones have suggested that ethene came from a surface-dependent reaction with a polycrystalline copper catalyst [4]. Studies have also been conducted on the chlorine-catalyzed pyrolyses by Ashmore and Owen [5], on the laser induced thermal decomposition by Dyer and Matthews [6], and on flat-flame burner decomposition by Kassem et al. [7]. These decomposition mechanisms studied by photo, laser, and thermal processes were correlated with the following reaction pathways [4–6]:

$$C_2H_4Cl_2 \rightarrow C_2H_4Cl^* + Cl \qquad \text{(thermal)} \tag{1a}$$

$$C_2H_4Cl_2 + h\nu \rightarrow C_2H_4Cl^* + Cl \qquad \text{(photo)} \tag{1b}$$

$$C_2H_4Cl^* \rightarrow C_2H_4 + Cl \tag{2}$$

$$C_2H_4Cl_2 + Cl \rightarrow C_2H_3Cl_2 + HCl \tag{3}$$

$$C_2H_3Cl_2 \rightarrow C_2H_3Cl + Cl \tag{4}$$

Since gas phase EDC has a large cross-section for electrons to attach, EDC could thus promptly decompose through the pathways listed as [4,8]:

$$C_2H_4Cl_2 + e^- \rightarrow C_2H_4Cl_2{}^{-*} \tag{5}$$

$$C_2H_4Cl_2{}^{-*} \rightarrow C_2H_4Cl + Cl^- \tag{6a}$$

$$C_2H_4Cl_2{}^{-*} \rightarrow C_2H_4Cl^- + Cl \tag{6b}$$

$$C_2H_4Cl_2{}^{-*} \rightarrow C_2H_4 + Cl_2{}^- \tag{6c}$$

Formation of Cl^- in (6a) was dominant and the $C_2H_4Cl_2{}^-$ ion was not observed in the analysis of EDC decomposition

---

[*] Corresponding author. Tel.: +886-6-275-7575x54520;
fax: +886-6-275-2790.
E-mail address: ctli@mail.ncku.edu.tw (C.-T. Li).

1385-8947/02/$ – see front matter © 2002 Elsevier Science B.V. All rights reserved.
PII: S1385-8947(02)00135-3

by negative ion mass spectroscopy. Acetylene was expected to be produced primarily from reactions as follows [8]:

$$C_2H_3Cl + Cl \rightarrow C_2H_2Cl + HCl \tag{7}$$

$$C_2H_2Cl \rightarrow C_2H_2 + Cl \tag{8}$$

Kassem and Senkan have conducted an EDC combustion study [9]. Highly chlorinated hydrocarbons such as C_2Cl_4, C_2HCl_3, *trans*-$C_2H_2Cl_2$, C_2HCl, CCl_4, and $CHCl_3$, as well as Cl_2 and $COCl_2$ were detected. However, no CH_2Cl_2 was found in that study.

Even more relevant to this paper is the work that has been done with radio frequency (rf) plasma. The rf plasma, known as cold plasma, is a branch of nonequilibrium plasma [10]. The temperature of the gas molecule in an rf plasma reactor is near room temperature, while the temperature of the electron will be higher than 10^4 K. The kinetic energy of an electron is much greater than that of a molecule in the cold plasma system. Therefore, the conventional reaction that needs to proceed at a very high temperature under normal conditions can be finished at a lower temperature in the cold plasma system [11]. In our previous study, dichloromethane (DCM) was decomposed in rf plasma [12]. Products species of CO, CO_2, H_2O, HCl, $CHCl_3$, CCl_4, $COCl_2$, C_2HCl_3, and C_2Cl_4 were detected. The fraction of total carbon input converted into CO_2 and CO was investigated. Hsieh et al. have conducted an examination of methyl chloride using Ar/O_2 rf plasma [13]. The decomposition fraction could reach as high as 99.99% and the species detected in the effluent gas stream included CO, CO_2, H_2O, HCl, CH_4, C_2H_2, C_2H_4, C_2H_6, C_2H_3Cl, C_2H_5Cl, and $COCl_2$. Phosgene formation was found by Lee et al. in an rf plasma reactor in which 1,1-$C_2H_2Cl_2$ was decomposed [14]. Decomposition mechanism and formation of $COCl_2$ were illustrated in that research.

In this work, rf plasma was used to decompose EDC. Decomposition fraction of EDC [$\eta_{C_2H_4Cl_2}$, $(C_{in} - C_{out})/C_{in} \times 100\%$] and operational parameters such as power input and equivalence ratio [$\phi = (C_2H_4Cl_2/O_2)_{actual} \times (O_2/C_2H_4Cl_2)_{stoichiometric}$] were investigated. Attention was also given to the competition between DCM and EDC in the plasma system. In addition, the reaction mechanism of EDC decomposition was discussed.

2. Experimental

The main components of the experimental system are displayed in Fig. 1. The plasma reactor had a diameter of 4.14 cm and a height of 15 cm. External electrodes, 6.52 cm in height, were wrapped on the plasma reactor and grounded (Fig. 2). A plasma generator (Model ACG-10) and a matching network (Model MW-10) supplied 13.56 MHz rf power to the electrodes. Before starting the experiment, the EDC was stored in liquid nitrogen and the reactor was evacuated to 0.1–0.5 Torr by a vacuum pump (AICATEL 2033). Then a diffusion pump was used to keep the system pressure lower than 0.001 Torr for the cleanup of contamination. Finally, the liquid nitrogen was removed and the EDC gas

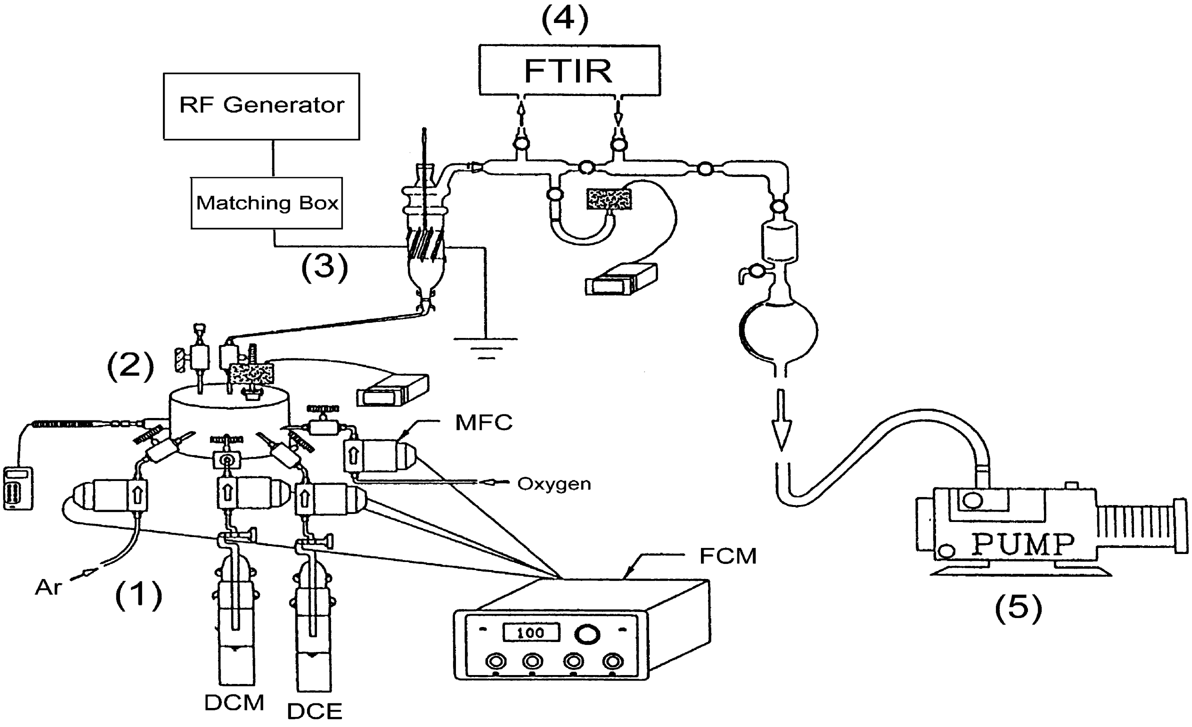

Fig. 1. Scheme of plasma system: (1) gas introduction device; (2) gas mixing system; (3) rf reactor and power supply system; (4) FTIR analysis system; and (5) vacuum pump.

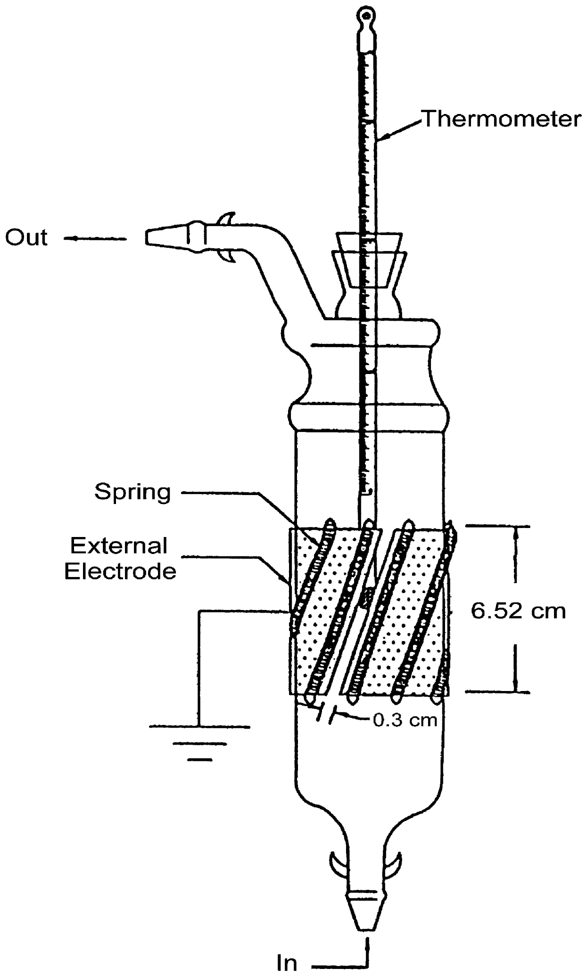

Fig. 2. The rf plasma reactor with external brass electrodes.

was introduced into a mixing system at room temperature. Ar/O_2 were selected as carrier/auxiliary gases. Mass flow controllers, obtained from Tylan Corp., were used to control gases flow rate. Influent gases were mixed in a stainless steel tank and then introduced from the bottom of the reactor. This arrangement ensured that all gases flowed through the glow discharge. The product species were examined on-line by a Fourier transform infrared (FTIR) spectrometer (Bio-Rad, Model FTS-7) for identification and quantification. Standard gases were used to calibrate gaseous reactants and product species. Standards that were in a liquid state at room temperature were injected into the preheated (150 °C) argon filled (750 Torr) mixing system. After the pressure had reached steady state, then the mixing system was filled with argon to 995 Torr. The ideal gas formula $PV = nRT$ was then used to calculate the standard gas concentration. Comparison of the response of peak height of standard gas at the same IR wave number yielded quantitation of the product species. All experiments were repeated at least three times and the averaged data were presented in the results.

3. Results and discussion

3.1. Effect of input power

The essential mechanisms in plasma include excitation, relaxation, ionization and recombination. To maintain a steady state of electron and ion densities, the ionization process must balance the recombination process. That means an external energy source is required [15]. At lower energy, most of the species are uncharged, ground state, or long lived excited state molecules. But at a higher input of power,

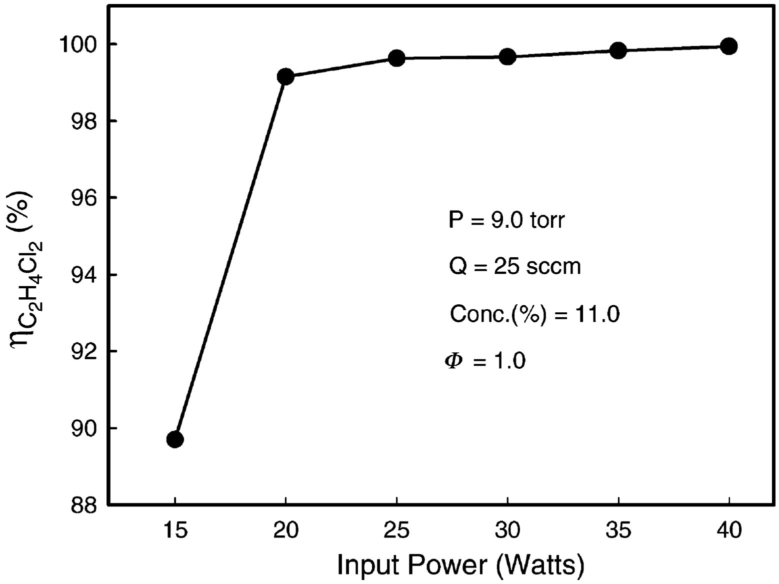

Fig. 3. Correlation between input power and EDC decomposition fraction.

the large consumption of energy could be a concern [16]. Experiments were conducted to determine the dependence of the $\eta_{C_2H_4Cl_2}$ on input power. Operational parameters were designed as follows: argon was used as the carrier gas, EDC feed concentration was 11%, input power ranged from 15 to 40 W, operational pressure was controlled at 9 Torr, the ϕ value was 1.0, and total gas flow rate was 25 sccm. Fig. 3 illustrated that the $\eta_{C_2H_4Cl_2}$ increased from 89.16 to 99.15% with input power from 15 to 20 W, respectively. As input power higher than 25 W, the $\eta_{C_2H_4Cl_2}$ reached a steady state of approximately 99.8%. Under higher power input, more effective collision frequency among the reactants, exciting argon, and free electron would occur [16] and resulted in a higher EDC decomposition fraction.

In order to evaluate the product distribution and the fraction of total input carbon converted into CO_2 and CO, higher input power (from 40 to 80 W) was used and other operational parameters were kept the same. Fig. 4A illustrated that with higher power input, more effluent concentrations of HCl, CO, and CO_2 were observed. In Fig. 4B, the mole fraction profiles of CCl_4, C_2HCl_3, C_2H_2, C_2H_4, and C_2H_6 were all decreased with input power. When it was as high as 80 W, C_2H_2, C_2H_4, and C_2H_6 were disappeared and converted into CO_2 and CO. All trace species such as C_2HCl_5, C_2H_3Cl, $CHCl_3$, C_2Cl_4, and $COCl_2$ vanished when input power was higher than 70 W (Fig. 4C). Specifically, increasing input power inhibited the formation of $COCl_2$. That is, formation of stable products like CO_2, CO, and HCl

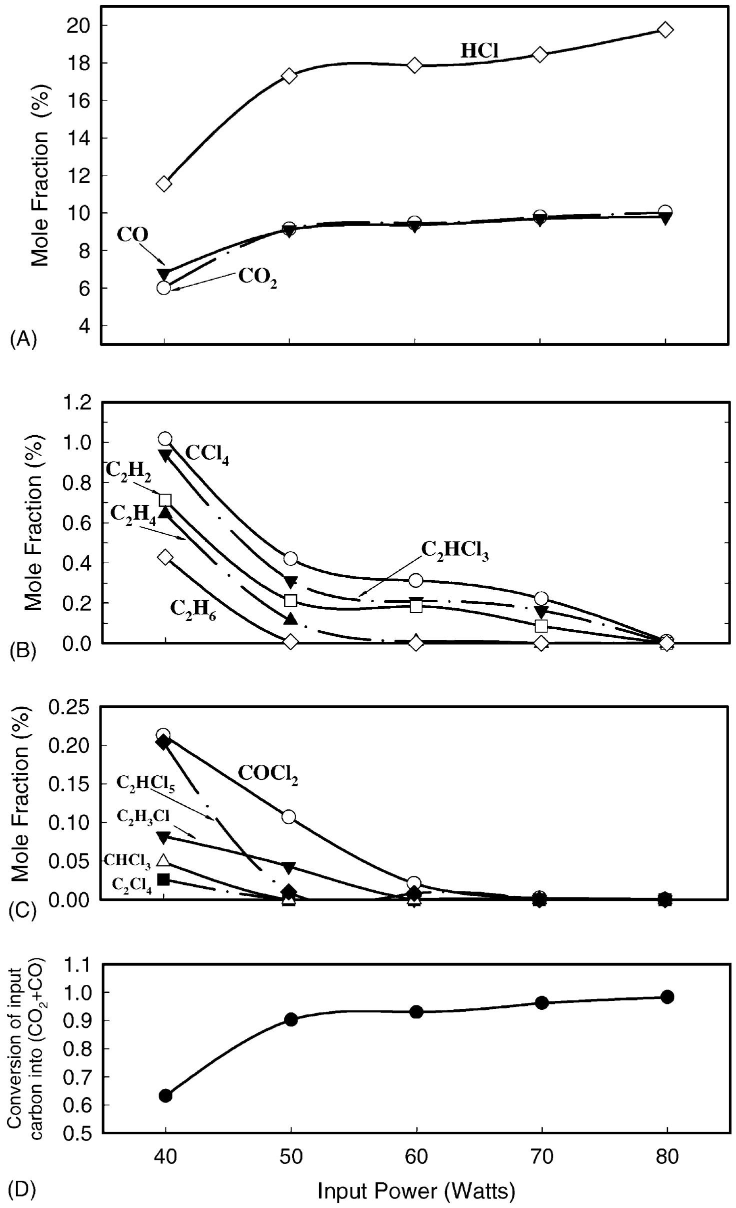

Fig. 4. Effect of input power on mole fraction of product species (A–C) and the fraction of total input carbon converted into CO_2 and CO (D).

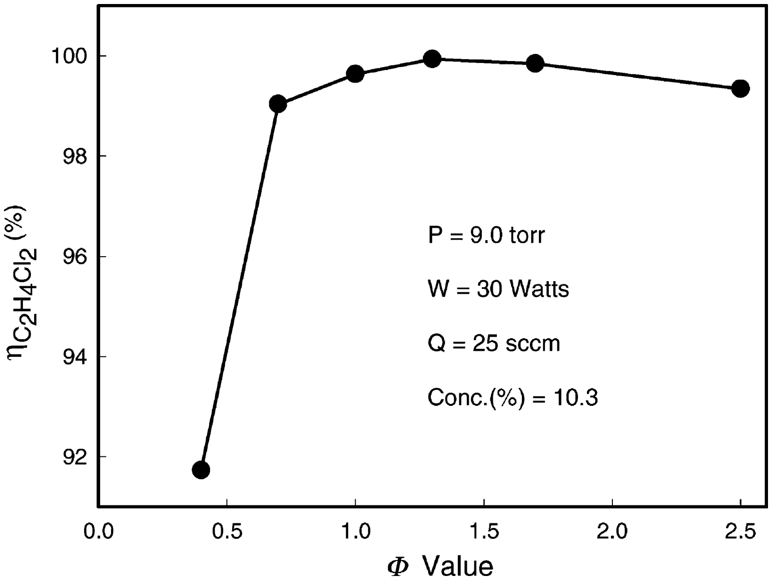

Fig. 5. Correlation between ϕ value and EDC decomposition fraction.

would replace product species like $COCl_2$ under higher input power. The mole fraction of total input carbon converted into [CO_2 + CO] increased from 63.3 to 90.3% with input power from 40 to 50 W, respectively. The values reached a steady state at power values higher than 50 W (Fig. 4D). Under higher input power, thermodynamically stable products such as CO and CO_2 dominated the conversion fraction of input carbon.

3.2. Effect of equivalence ratio

In this investigation, equivalence ratio was between 0.4 and 2.5, input power was 30 W, EDC feed concentration was 10.3%, operational pressure was 9 Torr, total gas flow rate was 25 sccm, and argon was used as the carrier gas.

The $\eta_{C_2H_4Cl_2}$ increased from 91.73 to 99.03% with the ϕ value increasing from 0.4 to 0.7, respectively, and reached the maximum 99.93% decomposition fraction at the ϕ value of 1.3 (Fig. 5). Under higher ϕ value, the Ar/O_2 ratio is higher than that of lower ϕ value. Since the energy transfer efficiency of argon is much higher than that of oxygen [12], a higher ϕ value would result in a higher decomposition of EDC. That also led to higher mole fraction of major product species such as HCl, CO, and CO_2 (Fig. 6A) and total carbon input converted into [CO_2 + CO] (Fig. 6D). However, as the ϕ value kept increasing to 2.5, the $\eta_{C_2H_4Cl_2}$

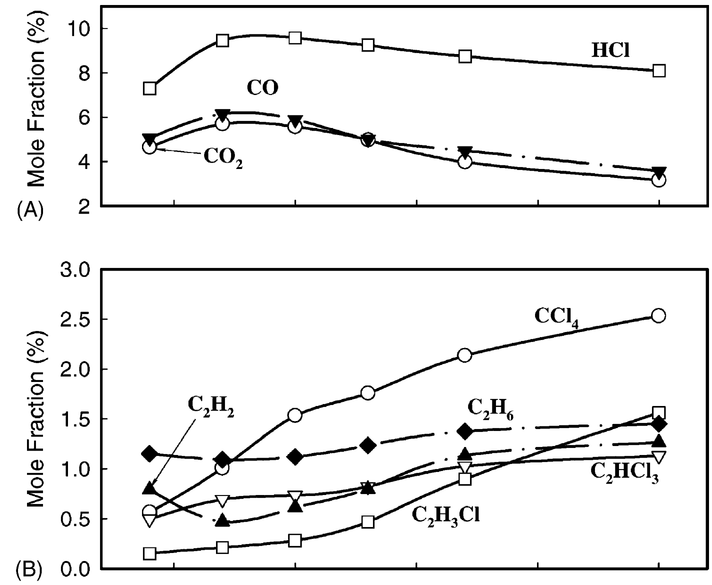

Fig. 6. Effect of ϕ value on mole fraction of product species (A–C) and the fraction of total input carbon converted into CO_2 and CO (D).

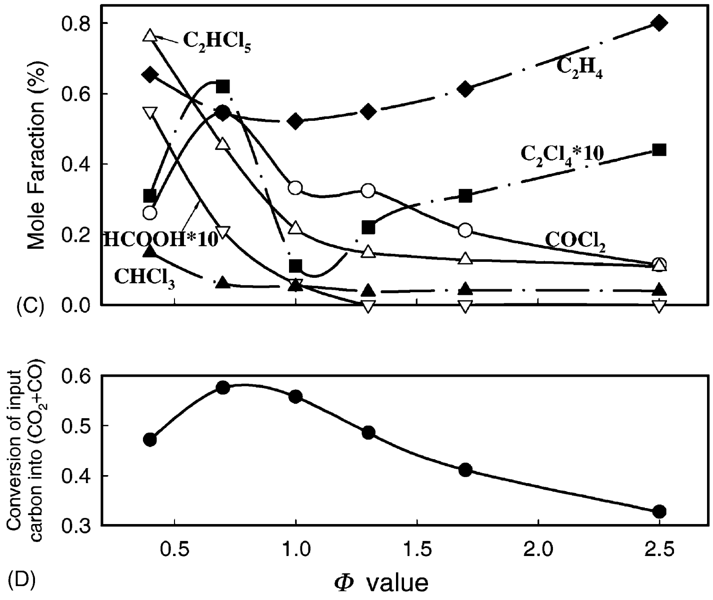

Fig. 6. (*Continued*).

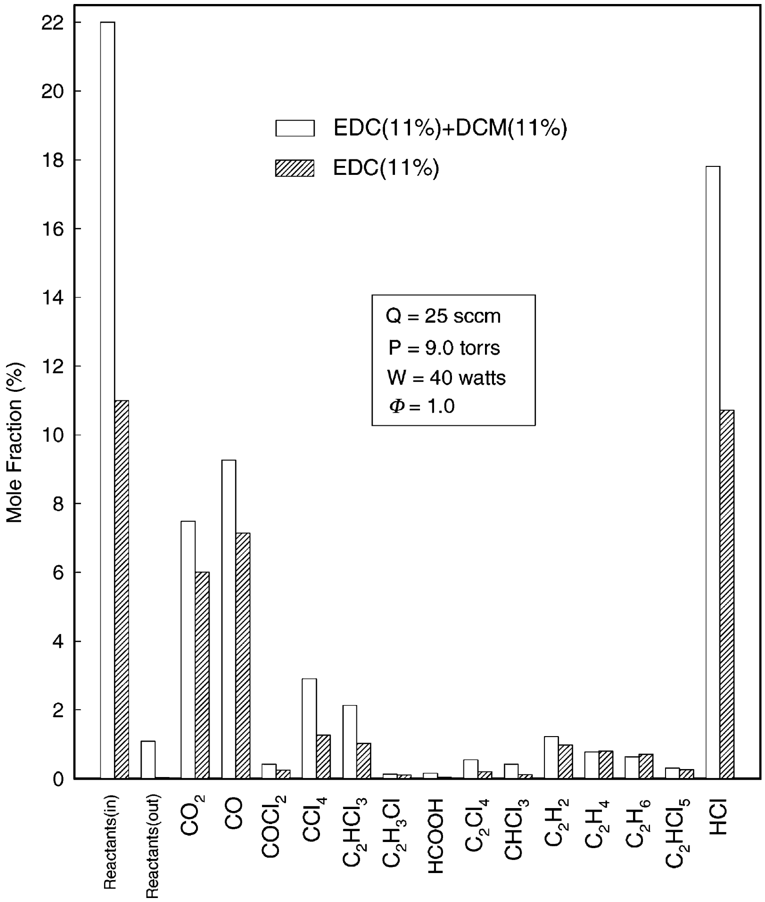

Fig. 7. Detected species of EDC (11%) and EDC (11%) + DCM (11%) decomposition.

decreased slightly to 99.34%. Meanwhile, the production of HCl, CO, and CO_2 (Fig. 6A) and total carbon input converted into $[CO_2 + CO]$ (Fig. 6D) were inhibited by less oxygen addition (high Ar/O_2 ratio). Specifically, this phenomenon was also observed in the formation of the $COCl_2$ (Fig. 6C). In addition to C and Cl, the formation of $COCl_2$ required oxygen supply. At a higher ϕ value, the feed oxygen was low and resulted in less $COCl_2$ formation. Meanwhile, as the ϕ value was higher than 1.0, more soot formation was found in the plasma reactor. Fig. 6B shows evidence of minor product species such as C_2H_2, C_2H_6, CCl_4, C_2HCl_3, and C_2H_3Cl. Those minor product species increased with the ϕ value, which the Ar/O_2 ratio was increased. Except for C_2H_4 and C_2Cl_4, trace product species such as C_2HCl_5, $COCl_2$, $CHCl_3$, and HCOOH all decreased with the ϕ value (Fig. 6C).

3.3. *EDC and DCM competition in plasma reactor*

Competition between EDC and DCM in plasma reactor had been studied under various influent concentrations such as EDC (11%), EDC (22%), and DCM (11%) + EDC (11%). Operational parameters were designed as follows: argon was used as the carrier gas, operational pressure was 9 Torr, the ϕ value was 1.0, input power was 30 W, and total gas flow rate was 25 sccm.

The decomposition fractions of both DCM and EDC within the DCM (11%) + EDC (11%) mixture were 94.78 and 95.34%, respectively. For independent influent concentration of EDC (22%) and EDC (11%), the decomposition fractions were 96.14 and 99.92%, respectively. Since the decomposition fractions of EDC (22%) and EDC (11%) were higher than that of DCM (11%) + EDC (11%) mixture, it indicated that the competition of DCM with EDC could affect the EDC decomposition. As illustrated in Fig. 7, EDC (11%) and DCM (11%) + EDC (11%) had the same product species. However, mole fractions of product species from DCM (11%) + EDC (11%) were higher than that of EDC (11%), except for C_2H_4 and C_2H_6. That due to decomposition of DCM did not contribute to the formation of C_2H_4 and C_2H_6. This result was consistent with our previous investigation that no nonchlorinated hydrocarbons were produced during the decomposition of DCM in rf plasma [12]. Fig. 8 shows that both the decomposition of EDC (22%) and DCM (11%) + EDC (11%) have the same product species. The mole fractions of product species of

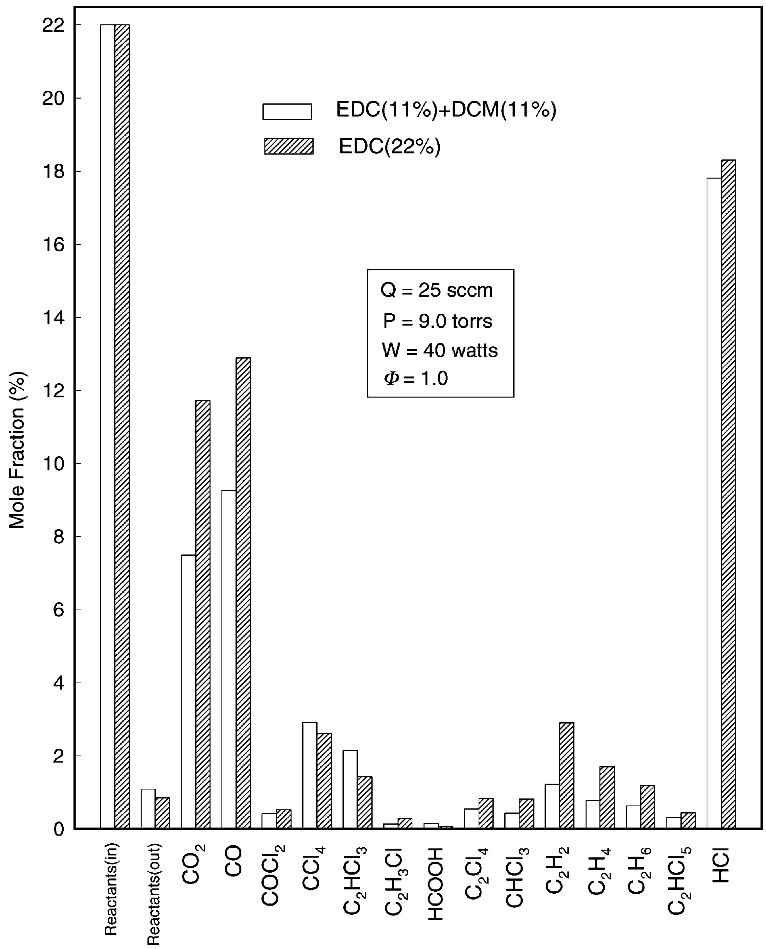

Fig. 8. Detected species of EDC (22%) and EDC (11%) + DCM (11%) decomposition.

EDC (22%) were higher than that of DCM (11%) + EDC (11%), except for CCl_4, C_2HCl_3, and HCOOH. Especially for C_2H_2, C_2H_4, and C_2H_6, the nonchlorinated hydrocarbon products from the decomposition of EDC (22%) were two times higher than that from DCM (11%) + EDC (11%) mixture. Comparing mole fractions of decomposition species among EDC (11%), EDC (22%), and DCM (11%) + EDC (11%), it confirmed that EDC was more decomposable than DCM and the competition of DCM with EDC would affected the decomposition fraction of EDC.

3.4. Possible reaction pathways for EDC decomposition

The EDC decomposition was mostly initiated by self-dissociation or by attack with the e^-, O, Cl, H, or OH. The possible reaction mechanism for EDC decomposition in a rf plasma system was listed as follows [4–6]:

$$C_2H_4Cl_2 + (h\nu,\ e^-) \rightarrow C_2H_4Cl^* + Cl + (e^-) \tag{1a$'$, 1b'}$$

$$C_2H_4Cl^* \rightarrow C_2H_4 + Cl \tag{2$'$}$$

$$C_2H_4Cl_2 + (O,\ Cl,\ OH) \rightarrow C_2H_3Cl_2 + (OH,\ HCl,\ H_2O) \tag{3$'$}$$

$$C_2H_3Cl_2 \rightarrow C_2H_3Cl + Cl \tag{4$'$}$$

$$C_2H_3Cl + (O,\ Cl,\ OH) \rightarrow C_2H_2Cl + HCl \tag{7$'$}$$

$$C_2H_2Cl \rightarrow C_2H_2 + Cl \tag{9}$$

$$C_2H_4Cl_2 + M \rightarrow 2CH_2Cl + M \tag{10}$$

$$C_2H_4Cl_2 + M \rightarrow CH_3 + CHCl_2 + M \tag{11}$$

After initiating the EDC decomposition, product species, using $CHCl_3$ for example, could be formed and decomposed as follows:

$$CHCl_2 + Cl = CHCl_3 \tag{12}$$

$$CHCl_2 + Cl_2 = CHCl_3 + Cl \tag{13}$$

$$CHCl_3 + (O,\ Cl,\ OH) = CCl_3 + (OH,\ HCl,\ H_2O) \tag{14}$$

Other effluent product species that was detected in this study could be invoked by a similar series of reaction mechanisms.

4. Conclusion

The species detected in the effluent stream of the EDC/O_2/Ar rf plasma included CO_2, CO, HCl, CCl_4, C_2HCl_3, C_2H_3Cl, C_2Cl_4, $CHCl_3$, C_2HCl_5, $COCl_2$, C_2H_2, C_2H_4, C_2H_6, and HCOOH. The decomposition fraction of EDC was dependent on the power input. When input power was as high as 80 W, stable products such as CO, CO_2 and HCl were dominant and other product species were inhibited. When the ϕ value increased from 0.4 to 0.7, a higher Ar/O_2 concentration ratio would result in a higher decomposition of EDC and led to higher mole fraction of stable product and the increment of total carbon input converted into [CO_2 + CO]. However, as the ϕ value kept increasing to 2.5, both the production of CO and CO_2 and the total carbon input converted into [CO_2 + CO] were hindered by less oxygen addition. As the ϕ value was higher than 1.0, soot formation was found in the plasma reactor. In the study of competition between DCM and EDC, EDC decomposed easier than DCM and DCM could affect the decomposition fraction of EDC.

References

[1] W.F. Carroll Jr., T.C. Berger, P.J. Borrelli, R.A. Garrity, R.A. Jacobs, J.W. Lewis, R.L. McCreedy, D.R. Tuhovak, A.F. Weston, Characterization of emissions of dioxins and furans from ethylene dichloride (DCE), vinyl chloride (VCM) and polyvinyl chloride (PVC), Chemosphere 37 (1998) 1957–1972.

[2] D.H.R. Barton, K.E. Howlett, The kinetics of the dehydrochlorination of substituted hydrocarbons. II. The mechanism of the thermal decomposition of 1,2-dichloroethane, J. Chem. Soc. (1949) 155.

[3] K.A. Holbrook, R.W. Walker, W.R. Watson, The pyrolysis of 1,2-dichloroethane, J. Chem. Soc. B (1971) 577.

[4] W.K. Walter, R.G. Jones, The reaction of 1,2-dichloroethane with copper, Catal. Lett. 24 (1994) 333.

[5] P.G. Ashmore, A.G. Owen, Chlorine-catalyzed pyrolysis of 1,2-dichloroethane, J. Chem. Soc. Faraday Trans. I 78 (1982) 677.

[6] P.E. Dyer, M. Matthews, KrF laser-induced thermal decomposition of 1,2-dichloroethane, J. Chem. Soc. Faraday Trans. 87 (1991) 2151.

[7] M. Kassem, M. Qun, S.M. Senkan, Chemical structure of fuel-rich 1,2-$C_2H_4Cl_2$/CH_4/O_2/Ar flame: effects of micro-probe cooling on the sampling of flames of chlorinated hydrocarbons, Combust. Sci. Technol. 67 (1989) 147.

[8] J.P. Johnson, L.G. Christophorou, J.G. Carter, Fragmentation of aliphatic chlorocarbons under low-energy ($\leq$10 eV) electron impact, J. Chem. Phys. 67 (5) (1977) 2196.

[9] M. Kassem, S.M. Senkan, Chemical structures of fuel-rich, premixed, laminar flames of 1,2-$C_2H_4Cl_2$ and CH_4, Combust. Flame 83 (3) (1991) 365.

[10] B. Eliasson, U. Kogelschatz, Nonequilibrium volume plasma chemical processing, IEEE Trans. Plasma Sci. 19 (1991) 1063.

[11] L.T. Hsieh, W.J. Lee, C.T. Li, M.B. Chang, H.C. Chang, Converting methane by using an rf plasma reactor, Plasma Chem. Plasma Process 18 (2) (1998) 215.

[12] C.T. Li, W.J. Lee, C.Y. Chen, Y.T. Wang, CH_2Cl_2 decomposition by using a radio-frequency plasma system, J. Chem. Technol. Biotechnol. 66 (1996) 382.

[13] L.T. Hsieh, W.J. Lee, C.T. Li, C.Y. Chen, Y.P.G. Wu, S.J. Chen, Y.F. Wang, Decomposition of methyl chloride by using an rf plasma reactor, J. Hazard. Mater. B 63 (1998) 69.

[14] W.J. Lee, C.Y. Chen, W.C. Lin, Y.T. Wang, C.J. Chin, Phosgene formation from the decomposition of 1,1-$C_2H_2Cl_2$ contained gas in an rf plasma reactor, J. Hazard. Mater. 48 (1996) 51.

[15] B.N. Chapman, Glow Discharge Processes, Wiley, New York, 1980, p. 49.

[16] H.F. Winters, Dissociation of methane by electron impact, J. Chem. Phys. 63 (1975) 3462.